BIOCHEMISTRY
including biophysical chemistry & molecular biology
Article

Biochemistry **2010,** *49,* 2087–2096 2087
DOI: 10.1021/bi901827k

The SV40 Large T-Antigen Origin Binding Domain Directly Participates in DNA Unwinding†

Erin C. Foster and Daniel T. Simmons*

Department of Biological Sciences, University of Delaware, Newark, Delaware 19716-2590

Received October 26, 2009; Revised Manuscript Received December 23, 2009

ABSTRACT: The origin binding domain (OBD) of SV40 large T-ag serves a critical role during initiation of DNA replication to position T-ag on the origin. After origin recognition, T-ag forms a double hexamer over the origin. Within each hexamer, the OBD adopts a lock washer structure where the origin recognizing A1 and B2 loops face toward the helicase domain and likely become unavailable for binding DNA. In this study, we investigated the role of the central channel of the OBD hexamer in DNA replication by analyzing the effects of mutations of residues lining the channel. All mutants showed binding defects with origin DNA and ssDNA especially at low protein concentrations, but only half were defective at supporting DNA replication *in vitro*. All mutants were normal in unwinding linear origin DNA fragments. However, replication defective mutants failed to unwind a small origin containing circular DNA whereas replication competent mutants did so normally. The presence of RPA and/or pol/prim restored circular DNA unwinding activity of compromised mutants probably by interacting with the separated DNA strands on the T-ag surface. We interpret these results to indicate a role for the OBD central channel in binding and threading ssDNA during unwinding of circular SV40 DNA. Mixing experiments suggested that only one monomer in an OBD hexamer was necessary for DNA unwinding. We present a model of DNA threading through the T-ag complex illustrating how single-stranded DNA could pass close to a trough generated by key residues in one monomer of the OBD hexamer.

Simian virus 40 is an excellent model system to study DNA replication due in part to the requirement of only one viral protein, large T-antigen (T-ag)[1] (*1*−*4*). T-ag is a 708 kDa multidomain protein comprised of three main functional domains: the N-terminal J-domain, the central OBD, and the C-terminal helicase domain. During replication, the functional form of T-ag is a double hexamer (DH) that orchestrates bidirectional DNA replication in the presence of host cell proteins (*5*−*8*). Electron microscopy has revealed the overall structure of T-ag in the presence of origin containing DNA to be a DH in a head to head orientation (*9*). Structures of various subdomains of T-ag have been solved including the N-terminal J-domain crystallized in complex with Rb (*10*), an NMR structure of the monomeric form of the OBD (*11*), and the crystal structure of dimeric (*12*) and hexameric OBDs (*13*) as well as several crystal structures of the hexameric helicase domain (*14*, *15*). However, the crystal structure of the complete DH or even an entire single hexamer remains elusive. The crystal structure of the helicase domain and EM imaging reveal that T-ag forms a ring-like structure with a central channel believed to be occupied by DNA during replication. The OBD hexamer is also ring-like (Figure 1), but in this case, it forms a lock washer structure with a gap between two monomers (*13*). Its central channel, which is also lined with hydrophilic and charged residues, may function similarly. In this study, we provide evidence that this channel may be occupied by ssDNA during SV40 DNA replication (as shown in Figure 9).

Other significant advantages of the SV40 model system include the single well-defined origin of replication and the minimal protein requirement for replication *in vitro*. The SV40 origin of replication consists of a central 23 bp perfect palindrome (site II) flanked on the early side by an imperfect palindrome (EP) and on the late side by an AT-rich track (*16*). T-ag is the only viral protein necessary for viral DNA replication serving as an initiator protein and as a bidirectional helicase (*6*−*8*, *17*). All other proteins needed are provided by the host cell. By fractionating cell extracts that support SV40 DNA replication *in vitro*, more than 10 host proteins were shown to participate in DNA replication (*18*−*21*). It was later determined that only three of these proteins are necessary for initiation of replication, including replication protein A (RPA), topoisomerase I (topo I), and the DNA polymerase α primase complex (pol/prim) (*22*−*27*). Multiple interactions among these proteins and T-ag are necessary for optimal initiation of SV40 DNA replication (*24*, *25*, *28*−*33*).

In order to initiate replication, T-ag must first recognize and bind to the core origin. The OBD is responsible for making specific interactions with four GAGGC pentanucleotide repeat sequences in the central palindrome of the origin using its A1 and B2 loops as previously described (*34*−*37*). T-ag then assembles into a double hexamer structure in the presence of ATP or ADP in a head to head orientation over the 64 bp core origin by a process that is not well understood. The double hexamer structure induces structural distortions in the flanking EP region and AT track of the origin in the absence of ATP hydrolysis (*38*, *39*). This is followed by bidirectional unwinding by the 3′ to 5′ helicase in an ATP-dependent manner (*40*, *41*). Cellular initiation factors are then recruited in a yet unclear process. RPA, topo I, and pol/prim

†This work was supported by USPHS Grant CA36118 to D.T.S.
*To whom correspondence should be addressed. E-mail: dsimmons@udel.edu. Tel: (302) 831-8547. Fax: (302) 831-2281.

Published on Web 01/28/2010

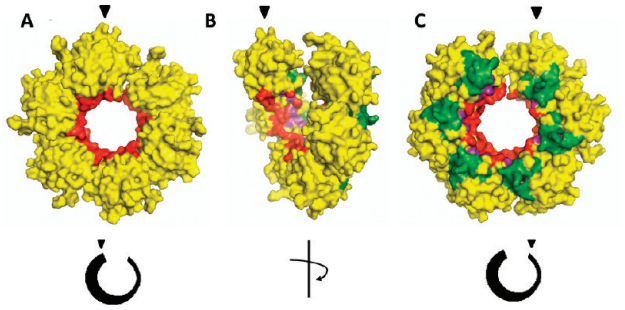

FIGURE 1: Residues lining the central channel of the OBD hexamer. Crystal structure of the OBD hexamer (*13*) modeled using PyMol v1.1 software (http://www.pymol.org/). Central channel residues are shown in red. A1 and B2 residues are shown in green and purple, respectively. (A) View of the double hexamer interface surface of the lock washer, (B) side view, and (C) view of the helicase proximal surface.

have all been shown to bind directly to T-ag, and these interactions are essential for initiation to occur maximally (*24*, *25*, *29*, *32*, *42*). The exact order of recruitment of these factors is still under investigation; however, previous evidence from our laboratory suggests that pol/prim and topo I bind first followed by RPA (*33*). RPA is needed to protect the exposed single strands and also to stimulate pol/prim (*30*, *43*). Topo I relieves supercoiling induced strain (*44*−*46*) and, by binding specifically to the C-terminal region of the helicase domain, stimulates the synthesis of RNA/DNA primers by pol/prim (*47*). After the initiation complex is formed and sufficient unwinding has occurred to expose the template strand for replication, the pol/prim enzyme comes into play. The primase subunit synthesizes an RNA primer, and polymerase α extends it with a short stretch of approximately 30 nucleotides of DNA thus completing initiation (*48*, *49*).

Unwinding and threading of DNA through the T-ag complex are essential to allow for replication to proceed. DNA unwinding is initiated at the C-terminal helicase domain in which one strand is displaced to the surface of the large tier while the other strand passes through the central channel of the hexamer (*50*). Various sites for the threading of the displaced strand back into the hexamer structure have been previously proposed, all of which include the passage of the strand near or through the OBD hexamer. EM imaging of double hexamers associated with origin DNA identified side channels at the junction of the OBD hexamers which were proposed to facilitate movement of DNA through the complex (*51*). Another group proposed the involvement of the A1 and B2 loops and the gap between terminal monomers to permit the passage of ssDNA (*52*). However, these two loops become reoriented toward the helicase domain when the OBD hexamerizes into a lock washer structure (*13*), limiting access of these loops to DNA. This reorientation raises the question of how the OBD interacts with DNA during unwinding. We investigated the possible role of the central channel of the OBD hexamer in DNA binding and unwinding by generating and analyzing single point mutants with substitutions of all central channel residues. We identified several mutants that were compromised in their ability to support DNA replication *in vitro* and also failed to normally unwind a circular origin-containing DNA. We propose that the normal residues participate in threading of ssDNA during DNA unwinding and describe a possible path of an unwound strand through the T-ag single hexamer.

EXPERIMENTAL PROCEDURES

Site-Directed Mutagenesis. Single-point substitutions were generated in SV40 large T-ag cDNA using the Stratagene QuikChange site-directed mutagenesis kit according to the manufacturer's recommendations. Mutations were generated in baculovirus transfer vector 941-T containing full-length T-ag cDNA (*53*). Briefly, synthetic oligonucleotides containing the desired mutation were annealed to denatured template plasmid DNA and extended by Pfu Turbo polymerase with a PCR. Unmutated plasmid DNA templates were degraded by *Dpn*I digestion for 1 h at 37 °C, and DNA was then used to transform XL Gold competent cells (Stratagene). Plasmid DNA was purified from ampicillin-resistant colonies by a mini-prep protocol (Promega). Purified DNA was confirmed for the correct mutation(s) by standard dideoxy sequencing using synthetic oligonucleotide primers.

Generation of Recombinant Baculoviruses. DNA confirmed for the correct substitution(s) was cotransfected with BaculoSapphire (Orbigen) DNA in *Spodoptera frugiperda* (Sf9) cells according to the manufacturer's instructions. T-ag-expressing recombinant viruses were screened by indirect immunofluorescence with anti-T monoclonal antibody PAb101 (*54*). Virus was then amplified in Sf9 cells (2×10^7 cells) prior to protein purification.

Protein Purification. Full-length wild-type and mutant T-ags were purified from baculovirus-infected High 5 insect cells by immunoaffinity chromatography with monoclonal PAb101 antibody-coupled Sepharose 4B beads as previously described (*28*). The antibody was covalently coupled to CNBr-activated Sepharose 4B beads (Pharmacia) as described by the manufacturer. After incubating cell lysates with antibody-containing beads and washing to remove unbound proteins, T-ag was eluted with ethylene glycol buffer (*55*) (50% ethylene glycol, 20 mM Tris-HCl (pH 8.5), 500 mM NaCl, 1 mM EDTA, 10% glycerol), dialyzed overnight against dialysis storage buffer (10 mM Tris-HCl (pH 8.0), 100 mM NaCl, 1 mM EDTA, 1 mM dithiothreitol, 50% (v/v) glycerol), and stored at −20 °C. The concentration of purified T-ag was determined by sodium dodecyl sulfate−polyacrylamide gel electrophoresis and Coomassie staining of the gel by comparison with a BSA standard. Purity was estimated to be greater than 95%.

Recombinant human RPA was expressed by IPTG induction of transformed *Escherichia coli* and purified by column chromatography as previously described (*56*).

Topoisomerase I was purified from infected Sf-9 insect cells as previously described (*46*).

Pol/prim was purified from baculovirus infected High-5 cells in a two-step process as previously described (*33*) using chitin affinity chromatography followed by chromatography on hydroxylapatite.

Oligomerization. Four hundred nanograms of T-ag was incubated in the presence or absence of 4 mM ATPγS (Alexis) in 30 μL of replication buffer (30 mM HEPES (pH 7.5), 7 mM $MgCl_2$, 40 mM creatine phosphate, 4 mM ADP, 1 mM dithiothreitol, 0.1 mg of bovine serum albumin/mL) for 10 min on ice followed by 30 min at 37 °C. Proteins were then cross-linked using a final concentration of 0.1% glutaraldehyde for an additional 10 min at 37 °C and diluted 2-fold in Laemmli loading buffer without β-mercaptoethanol or sodium dodecyl sulfate (*47*). T-ag oligomers were resolved on a 4−20% native polyacrylamide gradient gel in 0.05 M Tris (pH 8.8)−0.05 M glycine for 16 h at 100 V at 4 °C. T-ag was then detected by silver staining.

Table 1: Summary of Biochemical Properties of T-ag Point Mutants

residue and point mutation	activity as % of WT for protein concentration indicated[a]							
	oligomerization (1000 ng)	DNA replication (1000 ng)[b]	origin binding		ssDNA binding		DH formation (400 ng)	origin DNA fragment unwinding (600 ng)
			25 ng	400 ng	25 ng	400 ng		
177, Glu → Lys	+	±	±	+	−	+	+	+
178, Lys → Glu	+	−	−	±	−	−	++	+
178, Lys → Arg	+	++	±	+	±	+	+	+
179, Tyr → Phe	+	+	−	+	±	+	+	+
201, His → Phe	+	+	±	+	±	+	+	++
201, His → Asn	+	++	+	+	−	±	++	+
211, Tyr → Phe	+	±	±	+	±	+	+	+
214, Lys → Gln	+	±	±	+	±	+	+	+
214, Lys → Arg	+	±	−	±	±	+	+	++

[a]% WT activity is denoted as follows: (−) ≤25%; (±) 26−65%; (+) 66−99% (normal); (++) ≥100% (normal). [b]DNA replication assay using 293 cell extracts.

In Vitro DNA Replication Assay. Reactions were similar to those described by Trowbridge, Roy, and Simmons (*26*). Reactions (50 μL) contained 20 μL of 293 cell extract, 1 μg of T-ag, 100 ng of topoisomerase I, 200 ng of origin containing pSVO +11 (*18*), and 1 μCi of [^{32}P]dCTP in monopolymerase buffer (30 mM HEPES−KOH ([pH 8.0), 7 mM $MgCl_2$, 40 mM creatine phosphate, 4 mM ATP, 0.2 mM each CTP, GTP, and UTP, 0.1 mM each dATP, dGTP, and dTTP, 20 μM dCTP, 25 μg/mL creatine phosphokinase, 0.5 mM dithiothreitol, 50 μg/mL BSA). DNA was synthesized for 1 h at 37 °C, and the reaction was terminated by addition of stop buffer (0.02 M EDTA, 0.4% sodium dodecyl sulfate, 0.25 mg of proteinase K/mL final concentrations). After incubation for 30 min at 37 °C, labeled DNA was purified by phenol−chloroform extraction and filtration through a Centri-Spin20 column (Princeton Separation). DNA was separated on 1.5% agarose gels in Tris−borate−EDTA buffer (0.089 M Tris, 0.089 M boric acid, 0.02 M Na-EDTA) by electrophoresis for 5 h at 100 V. Gels were then dried and exposed to phosphor screens, and the labeled replicated DNA products were quantitated using a Molecular Dynamics PhosphorImager and ImageQuant 5.0 software.

DNA Binding Assay. The ability of T-ag to bind synthetic 64 bp core origin DNA and 55 nt nonspecific ssDNA was assessed using gel shift assays. ^{32}P end-labeled DNA substrates were generated as previously described (*50*). Binding reactions were carried out by incubating 25 or 400 ng of T-antigen with ^{32}P-labeled DNA substrate (2 ng of 64 bp DNA or 10 ng of ssDNA) in replication buffer for 30 min at 37 °C. The DNA−protein complexes were then cross-linked with 0.1% glutaraldehyde for an additional 10 min at 37 °C and subjected to electrophoresis at 25 mA for 3 h at 3 °C on a composite 2.5% acrylamide−0.6% agarose gel in Tris−borate−EDTA buffer. The gels were dried and exposed to phosphor screens (Molecular Dynamics). Binding activity was quantified by scanning the screens with a PhosphorImager (Molecular Dynamics) and by using ImageQuant 5.0 software.

For some mutants, ssDNA binding curves were generated by incubating increasing amounts of T-ag (4−1000 ng) with 2 ng of 55 nt ssDNA. The percent DNA bound was plotted against the corresponding concentrations of T-ag. Binding curves were obtained using BioDataFit 1.02 software (Chang Bioscience, Castro Valley, CA).

Origin DNA Unwinding Assay. Reactions include 600 ng of T-ag incubated with 2 ng of end-labeled 64 bp origin DNA in monopolymerase buffer for 1.5 h at 37 °C. Reactions were terminated by addition of stop buffer and incubated for another 30 min at 37 °C. Reactions were subjected to electrophoresis on a nondenaturing 7% acrylamide gel for 3 h at 110 V. Gels were dried and exposed to phosphor screens, and the labeled DNA was visualized with a Molecular Dynamics PhosphorImager and quantitated using ImageQuant 5.0 software.

Reactions were also performed with longer origin-containing fragments generated by PCR. All primer pairs included one oligonucleotide primer corresponding to the top strand residues 5188−5206 of SV40 DNA on the conventional map. The other primers corresponded to the bottom strand of SV40 DNA residues 15−41, 61−78, 79−94, and 95−114 in order to generate 97, 134p, 150, and 170 bp fragments, respectively. Three picomoles of each gel-purified PCR product was end-labeled with [γ-^{32}P]ATP. Thirty femtomoles of labeled product was included in unwinding reactions using similar conditions as described above for 64 bp unwinding.

Minicircle Unwinding Assay. ^{32}P-Labeled origin-containing 388 bp circular DNA was generated, and unwinding reactions were performed essentially as previously described (*47*). One nanogram of gel-purified ^{32}P-labeled circular DNA substrate was incubated with 400 ng of immnoaffinity-purified T-ag and 10 ng of topo I in monopolymerase buffer in a total reaction volume of 20 μL. For experiments with initiation factors, 200 ng of RPA and/or 50 ng of pol/prim were added to the above reaction mixture. For ssDNA competition experiments, 2 or 4 ng of 55 nt ssDNA was included in reactions containing T-ag, topo I, and pol/prim. After 1 h at 37 °C, the reactions were terminated by the addition of 5 μL of 2% SDS, 0.1 M EDTA, and 1 mg/mL proteinase K and incubated at 37 °C for 30 min. Samples were applied to composite gels containing 2.5% acrylamide and 0.6% agarose in Tris−borate−EDTA buffer and subjected to electrophoresis for 550 V·h at 3 °C. The gels were dried and exposed to a PhosphorImager screen.

RESULTS

Generation of Point Mutants. To investigate the function of the central channel of the OBD hexamer in DNA replication, we introduced single substitutions at each of the six residues that line the channel of the OBD hexamer spiral (Figure 1). Even though there is little sequence similarity at these sites among the DNA binding domains of other polyoma viruses, the SV40 T-ag and papilloma virus E1 proteins are structurally very similar (*11*, *13*),

suggesting common function. We made conservative and/or nonconservative changes at each site (Table 1). For instance, K178R represents a conservative substitution maintaining the charge, and K178E represents a nonconservative substitution reversing the charge. Mutations were introduced in the SV40 large T-ag gene using the Stratagene QuikChange site-directed mutagenesis protocol. Recombinant baculoviruses were generated by homologous recombination of plasmid DNA containing the mutant T-ag genes with BaculoSapphire (Orbigen) DNA in *S. frugiperda* (Sf9) cells. Wild-type and mutant T-ags were purified to 95% purity from baculovirus-infected High 5 insect cells with similar yields. Equivalent concentrations of mutant and WT T-ags were used in all assays.

Central Channel Mutants Oligomerize Normally. The ability of T-ag to oligomerize into hexamer and double hexamer structures is essential for DNA unwinding during replication (*36*, *57*). To ensure that mutant T-ags are structurally normal, we measured their ability to hexamerize in solution in the absence of DNA in an oligomerization assay. This process requires the presence of a nucleotide, in this case ATPγS. Although mutants showed some differences in their oligomerization patterns compared to WT, all mutants were able to form hexamers to a similar extent as WT (Table 1 and Supporting Information Figure 1). These results indicate that the overall structure of the mutant T-ags was not seriously affected.

Some Central Channel Mutants Are Defective in DNA Replication in Vitro. Next, we tested the effects of substitutions on the ability of mutants to promote DNA replication *in vitro* using a 293 cell extract system as previously described (*26*). Replication activity was measured by quantifying all labeled DNA products (Figure 2A). Mutants E177K, K178E, Y211F, K214Q, and K214R were significantly defective in supporting replication *in vitro* (Figure 2, Table 2). Charge reversal mutants K178E and E177K showed the least activity, with approximately 20% of WT, while Y211F, K214Q, and K214R displayed moderate activity varying from 50% to 62% of WT. Other substitutions such as the conservative change in K178R and mutations generated at H201 had little to no effect on the mutants' replication activity (Figure 2, Table 1).

Central Channel Mutants Have DNA Binding Defects. Since the OBD is known to be involved in DNA binding (*52*, *58*, *59*), we hypothesized that the central channel of the OBD hexamer interacts with DNA as well. We analyzed the ability of central channel mutants to bind a 64 bp origin DNA fragment (ori-DNA) using gel shift assays in the presence of ADP as previously described (*50*) (Figure 3A). ADP was used instead of ATP to prevent the loss of T-ag−DNA complexes caused by helicase activity. All mutants were normal in their ability to bind ori-DNA at the higher protein concentration; however, they showed some failure to bind at the lower concentration compared to WT T-ag especially E177K, K178E, Y179F, and K214R (Figure 3C). These normal residues are likely to be involved in nonspecific DNA binding since they are not known to be directly involved in origin recognition (*11*, *59*, *60*). These reaction conditions allow for formation of both single hexamers (SH) and double hexamers (DH) at low protein concentration whereas at a high concentration only double hexamers are generated (*61*, *62*). All mutants formed double hexamers normally at the higher protein concentration, providing further support for the structural integrity of mutant proteins (Table 1). Notably, the DNA binding defect seen in mutant Y179F did not interfere with DNA replication activity.

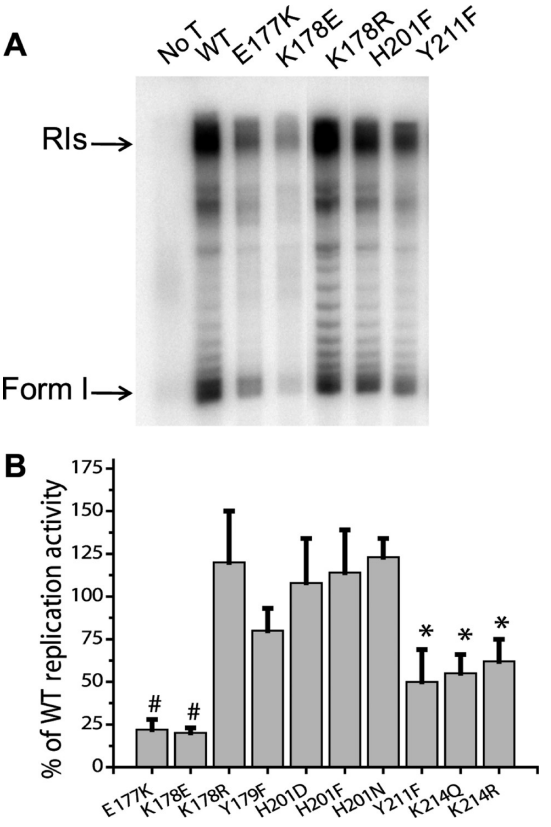

FIGURE 2: Mutations within the central channel of the OBD result in DNA replication defects. (A) Complete *in vitro* replication assay using WT or mutant T-ags and 293 cell extract in the presence of [α-^{32}P]dCTP. Newly synthesized DNA products were separated on a 1.5% agarose gel and visualized by autoradiography. The positions of replicative intermediates (RIs) and form I DNA are indicated. (B) Replication activity was measured by quantification of all labeled DNA products. Mutant activity is represented as a percentage of WT. *, $P \leq 0.05$, and #, $P \leq 0.01$, compared to WT activity.

Mutants were also tested for their ability to bind a 55 nt single-stranded oligonucleotide of random (nonorigin) sequence as previously described (*63*, *64*). The replication deficient mutants (E177K, K178E, Y211F, K214Q, K214R), previously shown to be defective in binding ori-DNA at low concentrations, showed similar defects in binding ssDNA at low protein concentrations (Figure 3B,D). Mutant K178E also failed to bind ssDNA normally at the higher concentration. Some replication competent mutants were also compromised in ssDNA binding at both low and high protein concentrations (H201N) or at low protein concentrations only (H201F) (Figure 3D and Table 1); however, these defects did not interfere with their ability to support DNA replication *in vitro*. To more completely assess the ability of replication-defective mutant proteins to bind ssDNA, binding curves were completed with increasing concentrations of T-ag (Figure 4A). T-ag-bound ssDNA was quantified, and percent binding at each T-ag concentration was used to obtain dose−response binding curves (Figure 4B). log EC_{50} values were calculated for each of the mutants from their respective binding curves using BioDataFit 1.02 software, and inverse values were compared as a percentage of WT (Figure 4C). All replication-deficient mutants were found to have a lower ability to bind to ssDNA with 20% or less of the WT inverse log EC_{50} value indicating moderate to severe defects. The percentages of ssDNA bound by mutant and WT T-ags in Figure 4 cannot be directly compared to those in Figure 3 because we used 5 times less DNA in the present experiment.

Table 2: Summary of Mutants' Replication and Unwinding Activities

	mean ± SD[a] calculated as percentage of WT activity				
mutant	DNA replication	minicircle unwinding	minicircle unwinding with RPA + pol/prim	Minicircle unwinding with pol/prim + 4 ng of ssDNA	group
WT	100	100	112 ± 5	82 ± 10	
K178R	120 ± 30	96 ± 13	N/D	N/D	1
Y179F	80 ± 13	97 ± 8	N/D	N/D	1
H201F	114 ± 25	100 ± 5	N/D	N/D	1
H201N	123 ± 11	90 ± 15	N/D	N/D	1
E177K	22 ± 6[b]	37 ± 2[c]	97 ± 10	22 ± 8	2
K178E	20 ± 3[b]	7 ± 2[b]	66 ± 13	5 ± 2	2
Y211F	50 ± 19[b]	74 ± 12	93 ± 6	N/D	2
K214Q	55 ± 11[c]	8 ± 2[b]	95 ± 10	13 ± 8	2
K214R	62 ± 13[c]	17 ± 7[b]	90 ± 13	18 ± 6	2

[a]Standard deviation determined from triplicate experiments. [b]Significant at $P \leq 0.01$. [c]Significant at $P \leq 0.05$. N/D indicates experiments not done.

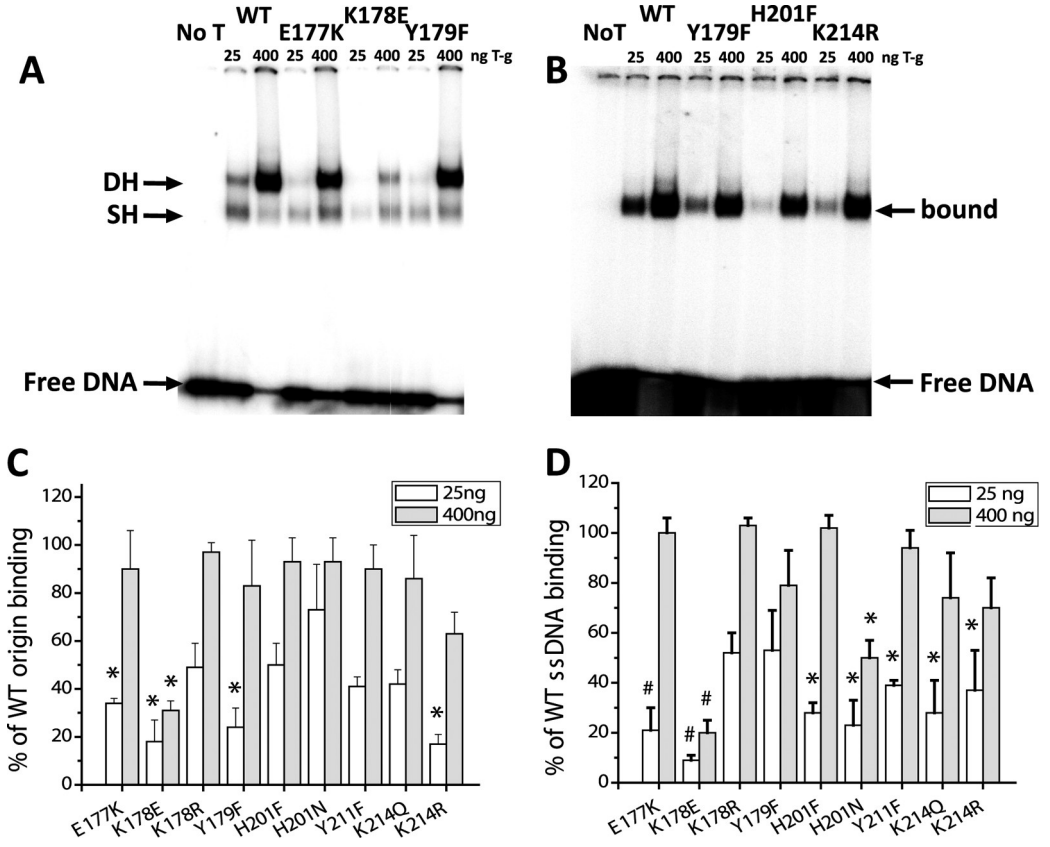

FIGURE 3: Central channel mutants display DNA binding defects. (A, B) Gel shift assays were used to test the binding of T-ag to DNA in the presence of replication buffer and ADP. DNA protein complexes were cross-linked and separated on a composite acrylamide−agarose gel. (A) Origin binding was tested using a 64 bp origin containing DNA fragment. (B) ssDNA binding was tested using a 55 nt oligonucleotide. (C) Origin binding was measured by quantifying both single hexamers (SH) and double hexamers (DH) and expressed as a percentage of WT activity. (D) Bound ssDNA complexes were quantified and represented as a percentage of WT activity. *, $P \leq 0.05$, and #, $P \leq 0.01$, compared to WT activity.

Central Channel Mutants Can Unwind Origin-Containing Linear DNA. After T-ag assembles into a double hexamer over the origin, its helicase activity is used to unwind the DNA (*61*, *63*, *64*). The mutants' origin-unwinding activity was evaluated using a 64 bp origin fragment DNA under normal assay conditions (600 ng of protein) as previously described (*31*, *50*). All mutants were normal in unwinding this DNA substrate (Supporting Information Figure 2 and Table 1). To test the possibility that these mutants fail to unwind longer DNAs, 97, 134, 150, and 170 bp origin DNA fragments were subjected to unwinding reactions. An example of an unwinding reaction with the 150 bp substrate is shown in Supporting Information Figure 2A. All mutants were also normal in unwinding all of these longer DNA fragments (Supporting Information Figure 2B). There was also no significant difference in the ability of K178E to unwind the 64 bp origin DNA compared to WT T-ag at various protein concentrations (Supporting Information Figure 3). These results therefore demonstrate that, in addition to forming normal amounts of double hexamers over the origin, the mutants' helicase activity is normal.

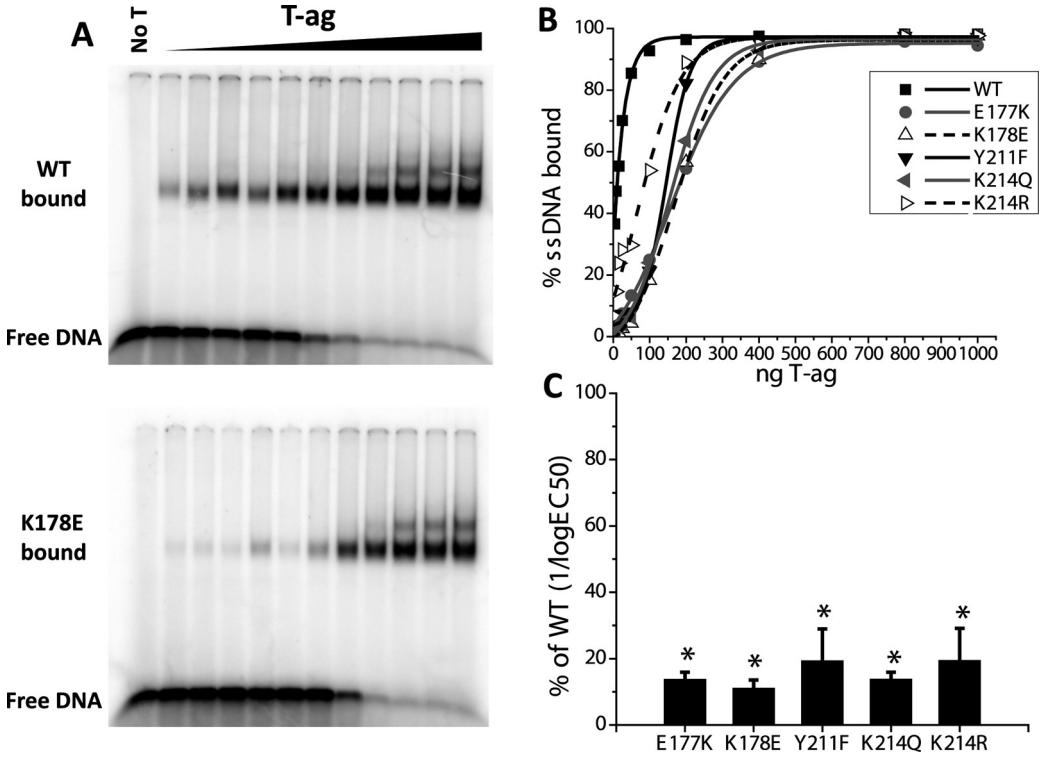

FIGURE 4: Replication deficient mutants display lower ability to interact with ssDNA. (A) ssDNA binding assays were performed using increasing amounts of T-ag (from 4 to 1000 ng) and a fixed amount (2 ng) of 55 nt ssDNA. DNA−protein complexes were cross-linked and run on a composite gel. Bound ssDNA complexes were quantified, and percent of DNA bound was calculated for each T-ag concentration. (B) Dose−response binding curves were generated for WT and replication deficient mutants using 4, 8, 16, 25, 50, 100, 200, 400, 800, and 1000 ng of T-ag. (C) log EC_{50} values were determined from representative binding curves using BioDataFit 1.02, and the inverse of the log EC_{50} value for each mutant was plotted as a percentage of WT. *, $P \leq 0.05$ compared to WT activity.

Replication-Deficient Mutants Are Unable to Unwind Circular DNA. Plasmid DNA is the substrate provided in the replication assay, and thus we wanted to evaluate the mutant's ability to unwind circular DNA. A 388 bp minicircle origin DNA was used as a substrate as previously described (*28*, *47*). Unwinding activity of WT and mutant T-ags was measured by quantitation of only the −5 underwound DNA, as previously characterized by Roberts (*65*). All replication-deficient mutants except for Y211F were compromised in their ability to form this underwound DNA product as compared to WT T-ag (Figure 5). Mutants K178E and K214Q showed the most defect with less than 10% unwinding activity whereas K214R and E177K were more active at 17% and 37%, respectively. Circular DNA unwinding defects correlated well with the inability of the mutants to support DNA replication *in vitro* (Table 2). The loss of unwinding activity did not result from an inability of mutants to bind the circular DNA substrate (Supporting Information Figure 4).

Mixing experiments were then carried out to analyze the impact of incorporating mutant monomers within a WT unwinding complex. The most defective mutant, K178E, was chosen for this experiment, in which different relative amounts (from 1:5 to 5:1) of mutant and WT T-ags were present in a total of 400 ng. We reasoned that mixing of subunits should occur equally to allow the formation of hexamers containing mutant and WT monomers since the mutations exist within the central channel of the OBD and do not prevent hexamerization. For each mutant: WT ratio, a distribution of complexes should form where the average structure should contain the ratio of molecules present in the reaction. Increasing relative amounts of mutant protein suppressed the unwinding reaction in a linear fashion (Figure 6),

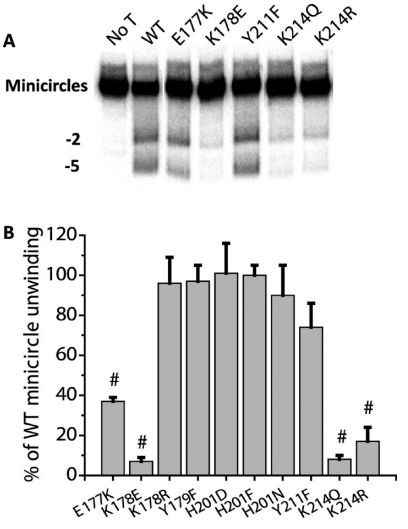

FIGURE 5: Replication deficient mutants are unable to support unwinding of a small circular DNA substrate. (A) 388 bp covalently closed origin containing circular DNA (minicircle) was subjected to unwinding reactions with WT or mutant T-ag and topo I in monopolymerase buffer. Underwound products were separated from the starting minicircles on composite gels. −2 and −5 underwound products were visualized as characterized by Roberts (*65*). Percent unwinding was quantified for the −5 supercoiled product only. (B) Unwinding activity of mutants was plotted as a percentage of WT. #, $P \leq 0.01$ compared to WT activity.

showing that the presence of mutant subunits inhibits unwinding in direct proportion to their relative amount.

Addition of Initiation Factors Recovers Unwinding Activity of Deficient Mutants. RPA is known to interact with both

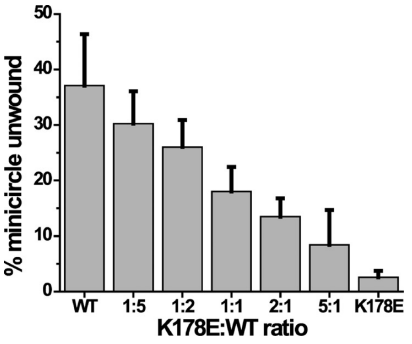

FIGURE 6: Minicircle unwinding by WT T-ag is linearly suppressed by addition of K178E mutant. Mixing experiments were performed using various ratios of WT and K178E T-ag to generate hexamers with increasing numbers of mutant monomers. Percent minicircle unwinding was calculated for each mixture by quantifying production of −5 supercoiled DNA products.

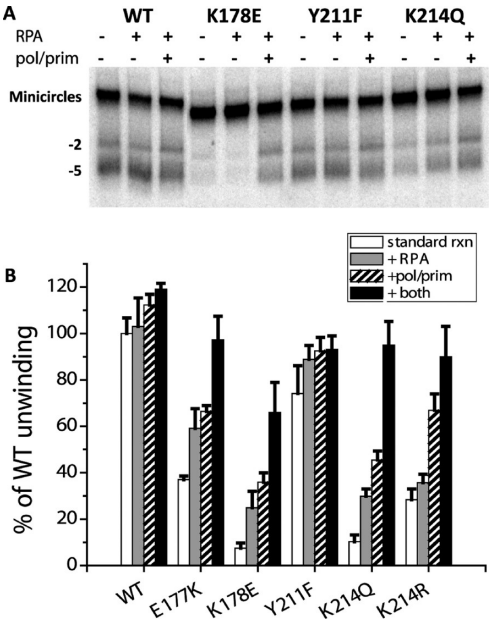

FIGURE 7: Addition of initiation factors recovers minicircle unwinding by deficient mutants. (A) RPA and/or pol/prim were added to standard minicircle unwinding reactions containing T-ag and topo I. Underwound products were separated on a composite gel, and formation of −5 supercoiled DNA products was quantified. (B) All values were normalized to that of WT T-ag in the absence of initiation factors (standard reaction).

the OBD and ssDNA exposed as a result of helicase activity (*25*, *30*, *43*). RPA may therefore aid unwinding by interacting with the unwound strand. Pol/prim has also been shown to stimulate binding and unwinding of origin containing DNA by T-ag under some conditions (*24*, *29*, *66*, *67*). With these findings in mind, minicircle unwinding reactions were performed in the presence of RPA and/or pol/prim to test whether the presence of these factors could rescue the mutants' circular DNA unwinding defect. The addition of either of these initiation factors or both together was able to stimulate the unwinding of the circular DNA substrate by mutant T-ags (Figure 7). RPA and pol/prim had little effect on unwinding by WT T-ag or unwinding positive mutant Y211F (Figure 7). Recovery of activity was most dramatic for the mutants having the greatest defect in the absence of initiation factors (K178E and K214Q). At the concentrations of proteins used, pol/prim stimulated mutant unwinding activity more than RPA, and both proteins together were able to restore almost normal levels of activity (Figure 7B and Table 2).

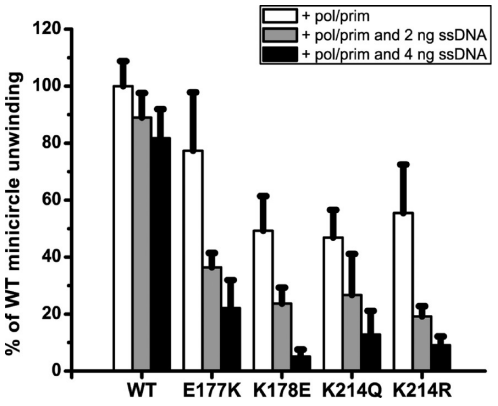

FIGURE 8: ssDNA added to minicircle unwinding reactions with deficient mutants compromises the stimulatory effect of pol/prim. Minicircle unwinding reactions were performed in the presence of pol/prim with or without 2 or 4 ng of 55 nt ssDNA. Unwinding activity was measured by the quantification of the −5 supercoiled DNA products and represented as a percent of WT activity without added ssDNA.

During replication, pol/prim interacts with the exposed ssDNA at the surface of the T-ag complex in order to synthesize the complementary strand (*24*, *68*). Thus, if pol/prim stimulation of circular DNA unwinding occurs due to an interaction with the displaced DNA, then it may be competed off the exposed strand by exogenously added ssDNA. Minicircle unwinding reactions were performed in the presence of pol/prim with or without 2 or 4 ng of competitor ssDNA. This represents a 14- and 28-fold molar excess of ssDNA over the circular DNA substrate, respectively. Quantitation of the −5 underwound products revealed that the presence of 2 ng of ssDNA in mutant unwinding reactions resulted in a partial block of the stimulation by pol/prim whereas 4 ng of ssDNA resulted in a complete loss of stimulation (Figure 8 and Table 2). WT T-ag was affected only slightly by the presence of the ssDNA competitor (Figure 8 and Table 2). These results imply that pol/prim stimulates DNA unwinding by interacting with the exposed ssDNA.

DISCUSSION

The properties of the mutants in this study are summarized in Tables 1 and 2. We demonstrated that mutation of four central channel residues within the OBD hexamer interfered with the ability of T-ag to bind DNA and to support DNA replication *in vitro*. The DNA binding defects did not, however, clearly correlate with an inability to participate in DNA replication. Interestingly, we found that there was an excellent correlation of loss of DNA replication with an inability to unwind circular SV40 DNA (Table 2). These data led to the classification of mutants into two main groups, those that support normal replication (group 1) and those that were impaired (group 2).

Group 1 mutants consist of K178R, Y179F, H201F, and H201N. These mutants were able to support DNA replication *in vitro*. Although DNA replication was not affected, the mutations lowered the ability to bind 64 bp ori-DNA and 55 nt nonspecific ssDNA (Table 1). It is possible that these mutants might show a DNA replication defect at low protein concentrations; however, this was not tested due to the difficulty in obtaining reproducible results under such conditions. In any case, these data support the idea that these central channel residues are important for DNA interactions.

Group 2 mutants consisting of E177K, K178E, Y211F, K214Q, and K214R were unable to support normal levels of DNA replication *in vitro*. Except for Y211F, these replication defects correlated with an inability to unwind circular origin-containing DNA (Figure 5 and Table 2). In contrast, they were normal in their ability to unwind linear origin-containing DNAs of various lengths (Supporting Information Figure 2) in spite of their ori-DNA and ssDNA binding defects at low protein concentrations (Figures 3 and 4). Therefore, we conclude that mutants have no difficulty in forming the functional double hexamer helicase over the origin and unwinding it in the context of a linear DNA fragment. The problem surfaces with circular DNA presumably because its topology imposes constraints on how the DNA molecule is unwound and threaded through the T-ag complex. Linear origin-containing fragments lack these constraints, and due to its flexible nature, there is less need for ordered interactions within the OBD hexamer during unwinding. The ends of linear DNA are free to writhe as necessary to relieve any superhelical tension induced by the unwinding process, and consequently, unwinding is less dependent on proper threading of the DNA through the T-ag double hexamer. Unwinding of covalently closed circular DNA, however, requires interactions within the central channel and elsewhere on the OBD to properly thread the unwound strands and allow for further unwinding to occur. Consequently, replication of circular plasmid DNA by group 2 mutants is compromised.

Initiation factors were able to rescue the mutants' unwinding activity (Figure 7 and Table 2). The most likely way this could take place is by interacting directly with the unwound DNA strands on the T-ag surface. This idea is supported by the finding that the presence of ssDNA in mutant unwinding reactions prevented the stimulatory effect of pol/prim (Figure 8, Table 2). RPA may aid in the threading process by pulling the ssDNA from the lock washer as previously proposed (*69*). It has also been suggested that origin unwinding is coupled to synthesis and elongation of primers by the association of polymerase α with T-ag and RPA (*70*). This might explain how the presence of both cellular factors stimulates DNA unwinding more than either one alone. Although RPA and pol/prim were able to recover circular DNA unwinding activity by group 2 mutants, the presence of these factors in the replication assays did not overcome their defect. One possibility is that the initiation factors are present in limiting amounts in the replication extracts. Another explanation is that the ability of these factors to stimulate unwinding can occur only in the absence of active DNA synthesis. We are presently investigating both of these possibilities.

Given all the data presented in this paper, we favor the interpretation that the replication-defective mutants are unable to properly thread and propel single-stranded DNA during origin unwinding from circular DNA. This could explain the mutants' defects in binding origin and ssDNAs at low protein concentrations (Figures 3 and 4) and their failure to properly unwind circular DNA as well as the ability of initiation factors to rescue the mutants' deficiency in circular DNA unwinding (Figures 5 and 7). Since excess ssDNA interfered with this stimulatory effect, these factors most likely promote unwinding by binding the displaced strands and in this way compensate for the mutants' inability to properly thread and propel the denatured ori-DNA through the T-ag hexamer. In what could be a similar process, bacteriophage T7 DNA polymerase was proposed to increase the rate of unwinding by the T7 helicase by preventing slippage of the helicase (*71*). It is therefore possible that loss of DNA binding results in DNA slippage during unwinding by our mutant T-ags but can be overcome by the presence of pol/prim and/or RPA.

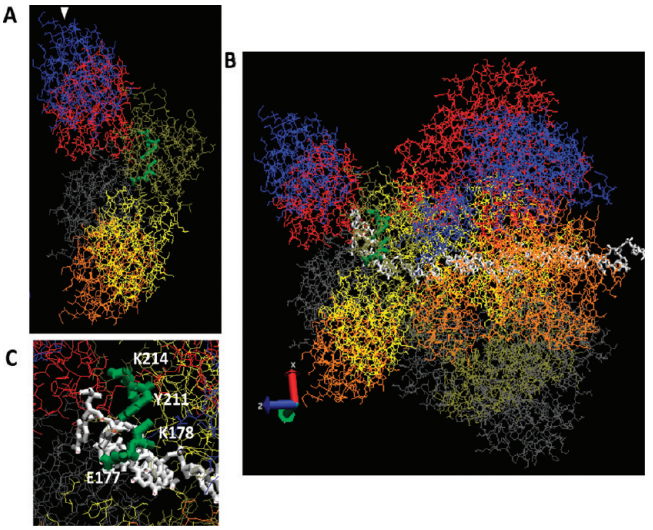

FIGURE 9: Model of ssDNA threaded through a trough generated by central channel residues within a single hexamer. (A) OBD spiral from Figure 1B was rotated slightly (arrow in Figure 1B identifies the same monomer in panel A). Different subunits of the OBD are shown in different colors. The trough generated by central channel residues E177, K178, Y211, and K214 is indicated in green on the tan-colored monomer. (B) The OBD spiral is in the same orientation as in (A) and is shown next to the hexameric helicase domain. The single strand of DNA moves from right to left and is shown in white. It is threaded through the helicase domain, bends, passes by the trough, and exits toward the viewer close to the gap of the OBD lock washer. (C) Blowup of part of (B) showing the trough in more detail.

Based on the extensive literature in this field and the data presented here, we constructed a model that illustrates the threading of single-stranded DNA through the T-ag single hexamer. Although several models of unwinding and threading have been proposed (*51*, *52*), none is totally consistent with all of the data. In our modeling, we came up with a number of related possibilities, and here we describe one such model. We combined the crystal structure of the hexamerized lock washer OBD (*13*, *69*) shown in Figure 1 with the hexameric helicase domain (*14*) in order to model a SH structure (Figure 9B). Results from mixing experiments also contributed to our model. We observed that mutant monomers suppressed WT minicircle unwinding activity in a linear fashion (Figure 6), suggesting that the central channel residues of only one OBD monomer are involved in the unwinding reaction. If all monomers in a hexamer were required, we would expect that incorporation of only one mutant monomer would poison the reaction and cause a severe drop in activity. Thus in our model, we considered that DNA passes by residues of only one monomer of the hexamer OBD structure. Our model shows the single-stranded DNA spooled through the helicase domain and exiting the T-ag SH complex near the gap of the OBD lock washer. This strand would then pass over the surface of the opposing hexamer in the DH (not shown).

The salient feature of the model is that the routed single strand passes very close to the residues that we have implicated in this study as being involved in DNA threading (E177, K178, Y211, and K214). Interestingly, these residues form a trough along the central channel surface of an OBD monomer that can accommodate ssDNA. The position of these residues is shown in green on the tan-colored monomer in side views of the OBD hexamer in Figure 9. The tan-colored OBD monomer is positioned at the gap

of the lock washer structure and is the closest monomer to the helicase domain. Figure 9B illustrates a hexamer of T-ag with a single strand of DNA passing by the residues of the trough and exiting toward the viewer. Figure 9C shows a close-up view of the ssDNA passing near the trough residues. Threading of ssDNA along the trough within this monomer would allow RPA and/or pol/prim to associate with the strand emerging from this structure to facilitate unwinding of circular DNA by mutant T-ags.

In conclusion, we presented evidence that the majority of the residues within the central channel of the OBD hexamer participate in ssDNA interactions suggesting that ssDNA passes through the central channel of the OBD during unwinding. Some mutants (group 1), although unable to properly interact with DNA, are not functionally affected and support DNA replication normally. Other mutants (group 2) are more severely affected and show defects in circular DNA unwinding and in DNA replication activities. The unwinding activity of these mutants is stimulated by the presence of initiation factors probably by binding directly to the separated strands of DNA. Altogether, our analysis suggests to us that the residues altered in the group 2 mutants function in sliding and threading of ssDNA during unwinding.

ACKNOWLEDGMENT

Special thanks to Rupa Roy and Weiping Wang for helpful discussion and technical support throughout this work.

SUPPORTING INFORMATION AVAILABLE

Supplemental data to support results presented here. This material is available free of charge via the Internet at http://pubs.acs.org.

REFERENCES

1. Bullock, P. A. (1997) The initiation of simian virus 40 DNA replication in vitro. *Crit. Rev. Biochem. Mol. Biol. 32*, 503–568.
2. Fanning, E., and Knippers, R. (1992) Structure and function of simian virus 40 large tumor antigen. *Annu. Rev. Biochem. 61*, 55–85.
3. Kelly, T. J. (1988) SV40 DNA replication. *J. Biol. Chem. 263*, 17889–17892.
4. Simmons, D. T. (2000) SV40 large T antigen functions in DNA replicationand transformation. *Adv. Virus Res. 55*, 75–134.
5. Smelkova, N. V., and Borowiec, J. A. (1997) Dimerization of simian virus 40 T-antigen hexamers activates T-antigen DNA helicase activity. *J. Virol. 71*, 8766–8773.
6. Li, J. J., and Kelly, T. J. (1984) Simian virus 40 DNA replication in vitro. *Proc. Natl. Acad. Sci. U.S.A. 81*, 6973–6977.
7. Stillman, B. W., and Gluzman, Y. (1985) Replication and supercoiling of simian virus 40 DNA in cell extracts from human cells. *Mol. Cell. Biol. 5*, 2051–2060.
8. Wobbe, C. R., Dean, F. B., Murakami, Y., Weissbach, L., and Hurwitz, J. (1986) Simian virus 40 DNA replication in vitro: study of events preceding elongation of chains. *Proc. Natl. Acad. Sci. U.S.A. 83*, 4612–4616.
9. Valle, M., Gruss, C., Halmer, L., Carazo, J. M., and Donate, L. E. (2000) Large T-antigen double hexamers imaged at the simian virus 40 origin of replication. *Mol. Cell. Biol. 20*, 34–41.
10. Kim, H. Y., Ahn, B. Y., and Cho, Y. (2001) Structural basis for the inactivation of retinoblastoma tumor suppressor by SV40 large T antigen. *EMBO J. 20*, 295–304.
11. Luo, X., Sanford, D. G., Bullock, P. A., and Bachovchin, W. W. (1996) Solution structure of the origin DNA-binding domain of SV40 T-antigen. *Nat. Struct. Biol. 3*, 1034–1039.
12. Meinke, G., Phelan, P., Moine, S., Bochkareva, E., Bochkarev, A., Bullock, P. A., and Bohm, A. (2007) The crystal structure of the SV40 T-antigen origin binding domain in complex with DNA. *PLoS Biol. 5*, e23.
13. Meinke, G., Bullock, P. A., and Bohm, A. (2006) Crystal structure of the simian virus 40 large T-antigen origin-binding domain. *J. Virol. 80*, 4304–4312.
14. Li, D., Zhao, R., Lilyestrom, W., Gai, D., Zhang, R., DeCaprio, J. A., Fanning, E., Jochimiak, A., Szakonyi, G., and Chen, X. S. (2003) Structure of the replicative helicase of the oncoprotein SV40 large tumour antigen. *Nature 423*, 512–518.
15. Gai, D., Zhao, R., Li, D., Finkielstein, C. V., and Chen, X. S. (2004) Mechanisms of conformational change for a replicative hexameric helicase of SV40 large tumor antigen. *Cell 119*, 47–60.
16. Deb, S., DeLucia, A. L., Baur, C. P., Koff, A., and Tegtmeyer, P. (1986) Domain structure of the simian virus 40 core origin of replication. *Mol. Cell. Biol. 6*, 1663–1670.
17. Wobbe, C. R., Dean, F. B., Murakami, Y., Borowiec, J. A., Bullock, P., and Hurwitz, J. (1987) In vitro replication of DNA containing either the SV40 or the polyoma origin. *Philos. Trans. R. Soc. London, Ser. B: Biol. Sci. 317*, 439–453.
18. Stillman, B., Gerard, R. D., Guggenheimer, R. A., and Gluzman, Y. (1985) T antigen and template requirements for SV40 DNA replication in vitro. *EMBO J. 4*, 2933–2939.
19. Wobbe, C. R., Weissbach, L., Borowiec, J. A., Dean, F. B., Murakami, Y., Bullock, P., and Hurwitz, J. (1987) Replication of simian virus 40 origin-containing DNA in vitro with purified proteins. *Proc. Natl. Acad. Sci. U.S.A. 84*, 1834–1838.
20. Wold, M. S., Weinberg, D. H., Virshup, D. M., Li, J. J., and Kelly, T. J. (1989) Identification of cellular proteins required for simian virus 40 DNA replication. *J. Biol. Chem. 264*, 2801–2809.
21. Malkas, L. H., Hickey, R. J., Li, C., Pedersen, N., and Baril, E. F. (1990) A 21S enzyme complex from HeLa cells that functions in simian virus 40 DNA replication in vitro. *Biochemistry 29*, 6362–6374.
22. Hubscher, U., Maga, G., and Spadari, S. (2002) Eukaryotic DNA polymerases. *Annu. Rev. Biochem. 71*, 133–163.
23. Collins, K. L., and Kelly, T. J. (1991) Effects of T antigen and replication protein A on the initiation of DNA synthesis by DNA polymerase alpha-primase. *Mol. Cell. Biol. 11*, 2108–2115.
24. Dornreiter, I., Copeland, W. C., and Wang, T. S. (1993) Initiation of simian virus 40 DNA replication requires the interaction of a specific domain of human DNA polymerase alpha with large T antigen. *Mol. Cell. Biol. 13*, 809–820.
25. Melendy, T., and Stillman, B. (1993) An interaction between replication protein A and SV40 T antigen appears essential for primosome assembly during SV40 DNA replication. *J. Biol. Chem. 268*, 3389–3395.
26. Trowbridge, P. W., Roy, R., and Simmons, D. T. (1999) Human topoisomerase I promotes initiation of simian virus 40 DNA replication in vitro. *Mol. Cell. Biol. 19*, 1686–1694.
27. Halmer, L., Vestner, B., and Gruss, C. (1998) Involvement of topoisomerases in the initiation of simian virus 40 minichromosome replication. *J. Biol. Chem. 273*, 34792–34798.
28. Gai, D., Roy, R., Wu, C., and Simmons, D. T. (2000) Topoisomerase I associates specifically with simian virus 40 large-T-antigen double hexamer-origin complexes. *J. Virol. 74*, 5224–5232.
29. Huang, S. G., Weisshart, K., Gilbert, I., and Fanning, E. (1998) Stoichiometry and mechanism of assembly of SV40 T antigen complexes with the viral origin of DNA replication and DNA polymerase alpha-primase. *Biochemistry 37*, 15345–15352.
30. Kenny, M. K., Lee, S. H., and Hurwitz, J. (1989) Multiple functions of human single-stranded-DNA binding protein in simian virus 40 DNA replication: single-strand stabilization and stimulation of DNA polymerases alpha and delta. *Proc. Natl. Acad. Sci. U.S.A. 86*, 9757–9761.
31. Khopde, S., and Simmons, D. T. (2008) Simian virus 40 DNA replication is dependent on an interaction between topoisomerase I and the C-terminal end of T antigen. *J. Virol. 82*, 1136–1145.
32. Murakami, Y., and Hurwitz, J. (1993) Functional interactions between SV40 T antigen and other replication proteins at the replication fork. *J. Biol. Chem. 268*, 11008–11017.
33. Simmons, D. T., Gai, D., Parsons, R., Debes, A., and Roy, R. (2004) Assembly of the replication initiation complex on SV40 origin DNA. *Nucleic Acids Res. 32*, 1103–1112.
34. Dean, F. B., Borowiec, J. A., Eki, T., and Hurwitz, J. (1992) The simian virus 40 T antigen double hexamer assembles around the DNA at the replication origin. *J. Biol. Chem. 267*, 14129–14137.
35. Dean, F. B., Borowiec, J. A., Ishimi, Y., Deb, S., Tegtmeyer, P., and Hurwitz, J. (1987) Simian virus 40 large tumor antigen requires three core replication origin domains for DNA unwinding and replication in vitro. *Proc. Natl. Acad. Sci. U.S.A. 84*, 8267–8271.
36. Mastrangelo, I. A., Hough, P. V., Wall, J. S., Dodson, M., Dean, F. B., and Hurwitz, J. (1989) ATP-dependent assembly of double hexamers of SV40 T antigen at the viral origin of DNA replication. *Nature 338*, 658–662.
37. Parsons, R. E., Stenger, J. E., Ray, S., Welker, R., Anderson, M. E., and Tegtmeyer, P. (1991) Cooperative assembly of simian virus 40

T-antigen hexamers on functional halves of the replication origin. *J. Virol. 65*, 2798–2806.
38. Borowiec, J. A., Dean, F. B., and Hurwitz, J. (1991) Differential induction of structural changes in the simian virus 40 origin of replication by T antigen. *J. Virol. 65*, 1228–1235.
39. Borowiec, J. A., and Hurwitz, J. (1988) Localized melting and structural changes in the SV40 origin of replication induced by T-antigen. *EMBO J. 7*, 3149–3158.
40. Goetz, G. S., Dean, F. B., Hurwitz, J., and Matson, S. W. (1988) The unwinding of duplex regions in DNA by the simian virus 40 large tumor antigen-associated DNA helicase activity. *J. Biol. Chem. 263*, 383–392.
41. Wiekowski, M., Schwarz, M. W., and Stahl, H. (1988) Simian virus 40 large T antigen DNA helicase. Characterization of the ATPase-dependent DNA unwinding activity and its substrate requirements. *J. Biol. Chem. 263*, 436–442.
42. Simmons, D. T., Melendy, T., Usher, D., and Stillman, B. (1996) Simian virus 40 large T antigen binds to topoisomerase I. *Virology 222*, 365–374.
43. Gomes, X. V., and Wold, M. S. (1996) Functional domains of the 70-kilodalton subunit of human replication protein A. *Biochemistry 35*, 10558–10568.
44. Champoux, J. J. (1992) Topoisomerase I is preferentially associated with normal SV40 replicative intermediates, but is associated with both replicating and nonreplicating SV40 DNAs which are deficient in histones. *Nucleic Acids Res. 20*, 3347–3352.
45. Stewart, L., Ireton, G. C., and Champoux, J. J. (1996) The domain organization of human topoisomerase I. *J. Biol. Chem. 271*, 7602–7608.
46. Stewart, L., Ireton, G. C., Parker, L. H., Madden, K. R., and Champoux, J. J. (1996) Biochemical and biophysical analyses of recombinant forms of human topoisomerase I. *J. Biol. Chem. 271*, 7593–7601.
47. Khopde, S., Roy, R., and Simmons, D. T. (2008) The binding of topoisomerase I to T antigen enhances the synthesis of RNA-DNA primers during simian virus 40 DNA replication. *Biochemistry 47*, 9653–9660.
48. Tsurimoto, T., and Stillman, B. (1991) Replication factors required for SV40 DNA replication in vitro. II. Switching of DNA polymerase alpha and delta during initiation of leading and lagging strand synthesis. *J. Biol. Chem. 266*, 1961–1968.
49. Murakami, Y., Wobbe, C. R., Weissbach, L., Dean, F. B., and Hurwitz, J. (1986) Role of DNA polymerase alpha and DNA primase in simian virus 40 DNA replication in vitro. *Proc. Natl. Acad. Sci. U.S.A. 83*, 2869–2873.
50. Wang, W., Manna, D., and Simmons, D. T. (2007) Role of the hydrophilic channels of simian virus 40 T-antigen helicase in DNA replication. *J. Virol. 81*, 4510–4519.
51. Valle, M., Chen, X. S., Donate, L. E., Fanning, E., and Carazo, J. M. (2006) Structural basis for the cooperative assembly of large T antigen on the origin of replication. *J. Mol. Biol. 357*, 1295–1305.
52. Reese, D. K., Meinke, G., Kumar, A., Moine, S., Chen, K., Sudmeier, J. L., Bachovchin, W., Bohm, A., and Bullock, P. A. (2006) Analyses of the interaction between the origin binding domain from simian virus 40 T antigen and single-stranded DNA provide insights into DNA unwinding and initiation of DNA replication. *J. Virol. 80*, 12248–12259.
53. Chen, L., Joo, W. S., Bullock, P. A., and Simmons, D. T. (1997) The N-terminal side of the origin-binding domain of simian virus 40 large T antigen is involved in A/T untwisting. *J. Virol. 71*, 8743–8749.
54. Gurney, E. G., Harrison, R. O., and Fenno, J. (1980) Monoclonal antibodies against simian virus 40 T antigens: evidence for distinct sublcasses of large T antigen and for similarities among nonviral T antigens. *J. Virol. 34*, 752–763.
55. Simanis, V., and Lane, D. P. (1985) An immunoaffinity purification procedure for SV40 large T antigen. *Virology 144*, 88–100.
56. Henricksen, L. A., Umbricht, C. B., and Wold, M. S. (1994) Recombinant replication protein A: expression, complex formation, and functional characterization. *J. Biol. Chem. 269*, 11121–11132.
57. Wessel, R., Schweizer, J., and Stahl, H. (1992) Simian virus 40 T-antigen DNA helicase is a hexamer which forms a binary complex during bidirectional unwinding from the viral origin of DNA replication. *J. Virol. 66*, 804–815.
58. Kim, H. Y., Barbaro, B. A., Joo, W. S., Prack, A. E., Sreekumar, K. R., and Bullock, P. A. (1999) Sequence requirements for the assembly of simian virus 40 T antigen and the T-antigen origin binding domain on the viral core origin of replication. *J. Virol. 73*, 7543–7555.
59. Simmons, D. T., Wun-Kim, K., and Young, W. (1990) Identification of simian virus 40 T-antigen residues important for specific and nonspecific binding to DNA and for helicase activity. *J. Virol. 64*, 4858–4865.
60. Simmons, D. T., Upson, R., Wun-Kim, K., and Young, W. (1993) Biochemical analysis of mutants with changes in the origin-binding domain of simian virus 40 tumor antigen. *J. Virol. 67*, 4227–4236.
61. Dean, F. B., Bullock, P., Murakami, Y., Wobbe, C. R., Weissbach, L., and Hurwitz, J. (1987) Simian virus 40 (SV40) DNA replication: SV40 large T antigen unwinds DNA containing the SV40 origin of replication. *Proc. Natl. Acad. Sci. U.S.A. 84*, 16–20.
62. Joo, W. S., Kim, H. Y., Purviance, J. D., Sreekumar, K. R., and Bullock, P. A. (1998) Assembly of T-antigen double hexamers on the simian virus 40 core origin requires only a subset of the available binding sites. *Mol. Cell. Biol. 18*, 2677–2687.
63. Jiao, J., and Simmons, D. T. (2003) Nonspecific double-stranded DNA binding activity of simian virus 40 large T antigen is involved in melting and unwinding of the origin. *J. Virol. 77*, 12720–12728.
64. Wu, C., Roy, R., and Simmons, D. T. (2001) Role of single-stranded DNA binding activity of T antigen in simian virus 40 DNA replication. *J. Virol. 75*, 2839–2847.
65. Roberts, J. M. (1989) Simian virus 40 (SV40) large tumor antigen causes stepwise changes in SV40 origin structure during initiation of DNA replication. *Proc. Natl. Acad. Sci. U.S.A. 86*, 3939–3943.
66. Abbate, E. A., Berger, J. M., and Botchan, M. R. (2004) The X-ray structure of the papillomavirus helicase in complex with its molecular matchmaker E2. *Genes Dev. 18*, 1981–1996.
67. Murakami, Y., and Hurwitz, J. (1993) DNA polymerase alpha stimulates the ATP-dependent binding of simian virus tumor T antigen to the SV40 origin of replication. *J. Biol. Chem. 268*, 11018–11027.
68. Matsumoto, T., Eki, T., and Hurwitz, J. (1990) Studies on the initiation and elongation reactions in the simian virus 40 DNA replication system. *Proc. Natl. Acad. Sci. U.S.A. 87*, 9712–9716.
69. Bochkareva, E., Martynowski, D., Seitova, A., and Bochkarev, A. (2006) Structure of the origin-binding domain of simian virus 40 large T antigen bound to DNA. *EMBO J. 25*, 5961–5969.
70. Dornreiter, I., Erdile, L. F., Gilbert, I. U., von Winkler, D., Kelly, T. J., and Fanning, E. (1992) Interaction of DNA polymerase alpha-primase with cellular replication protein A and SV40 T antigen. *EMBO J. 11*, 769–776.
71. Stano, N. M., Jeong, Y. J., Donmez, I., Tummalapalli, P., Levin, M. K., and Patel, S. S. (2005) DNA synthesis provides the driving force to accelerate DNA unwinding by a helicase. *Nature 435*, 370–373.